A one-pot synthesis of Fe-doped cryptomelane type octahedral molecular sieve manganese oxide for degradation of methylene blue dye

Amir Awaluddin[1*], *Riska* Anggraini[1], *Siti* Saidah Siregar[1], *Muhdarina*[1], and *Prasetya*[2]

[1]Department of Chemistry, Universitas Riau, Pekanbaru, Indonesia
[2]Department of Chemistry, Universitas Muhammadiyah Riau, Pekanbaru, Indonesia

Abstract. The Fe-doped octahedral molecular sieve manganese oxides have been successfully synthesized by one-pot synthesis of the reaction between $KMnO_4$ and glucose using sol-gel methods. The oxide products are then characterized by various techniques such as X-ray diffraction, scanning electron microscopy, atomic absorption spectroscopy and average oxidation state (AOS) of manganese in manganese oxides. The as-synthesized manganese oxide and Fe-doped manganese oxides are used as catalysts for the degradation of methylene blue dye using hydrogen peroxide as oxidants. The results indicated that the Fe-doped manganese oxide catalyst displayed much enhanced catalytic activities compared to undoped manganese oxide for methylene blue degradation. The differences in catalytic activities have been correlated with the difference in surface properties and crystallinity.

1 Introduction

The use of synthetic dyes as coloring agents has increased tremendously over the past few decades due to the rapid production of dye materials. Over 100,000 synthetic dyes are being used for the dyeing process, and the number continues to grow significantly every year. The synthetic dyes are replacing the role of natural dyes in most society as the dyes are more resistant to the environment, have a brighter color, inexpensive and easy to use factor. The effluents from these dye industries contain various toxic and hazardous chemicals that require an appropriate treatment before being released into the aquatic environment [1]. Thus, it is urgent to discover highly effective ways to overcome these severe problems.

The various strategies have been proposed for handling the dye wastes, which are mainly classified into three categories, namely biological, physical and chemical treatments. The use of biological approach is advantages in term of low-cost and environmentally friendliness but suffer from time-consuming and inapplicable for some dyes which are very toxic to the microorganisms. The physical methods such as adsorption, on the other hand, are a simple and widely efficient method for dye removal. However, most physical methods create second solid pollutant as most residual dyes in water are

* Corresponding author: amirawaluddin01@gmail.com

transferred into the adsorbent. Fenton process-based advanced oxidation process is an emerging prospect for dye removal by generating highly reactive and non-selective radicals for rapid degradation of organic contaminants such dyes. The traditional Fenton reaction is a catalytic process based on the reaction between the Fe^{2+} homogeneous catalyst and hydrogen peroxide (oxidant). The reactions generate various reactive radicals such as •OH, O_2•-, and HO_2•, but the •OH radical is known to be the most reactive one, which is the second strongest oxidant after fluorine. The drawback for the traditional Fenton process involves the narrow working pH window and only effective in the acidic condition. It also requires additional post-treatment after the complete dye degradation achieved since the catalyst dissolves in the final products.

The heterogeneous catalysts based on transition metal oxides having comparable catalytic activity with the homogeneous one for dye removal have gained a lot of attention. Among these, manganese oxides with tunnel or layer structures are considered to be as a promising catalyst candidate for dye removal. The tunnel structures of manganese oxides are constructed from edge-sharing and/or corner sharing of basic MnO_6 octahedra units, generating 1x1 tunnel (pyrolusite), 2x2 tunnel (cryptomelane), and 3x3 tunnel (todorokite). The tunnel manganese oxides are widely known as an octahedral molecular sieve (OMS), and cryptomelane is also known as an octahedral molecular sieve (OMS-2). These unique tunnel and layer structures together with excellent surface properties of manganese oxides make the oxides so unusual for a wide range of applications as a catalyst, adsorbent, ion-exchanges, battery, and electrochemical capacitors. The cryptomelane-type manganese oxide synthesized using hydrothermal method have been reported as a catalyst in the Fenton process for degradation of methylene blue (MB)[2].

The catalytic activity of cryptomelane can be improved by altering of a small fraction of Mn in the manganese oxides with other transition metals (known as doping), as reported by Ma et al. [3]. The resulting doped cryptomelane has the different chemical bonding from the pure cryptomelane mainly arise from the different interaction between dopant atom with oxygen atom compared to Mn with an oxygen atom in the cryptomelane. At the present study, we report the synthesis of Fe-doped cryptomelane manganese oxides catalysts using a simple approach by the reacting whole reactants including dopant in the single step. The whole reaction processes are known as a sol-gel method since the sol and gel are generated during the process. These as-prepared catalysts are subsequently applied to the degradation of MB. The choice of Fe^{2+} ion as the dopant in this study is based on the fact that the traditional Fenton processes are using Fe^{2+} as a homogeneous catalyst and proven to be active for MB degradation. It is interesting to know the effect of Fe^{2+} inserted into the framework of cryptomelane using this simple strategy for the catalytic degradation of MB. This easy and simple one-pot approach using sol-gel method for the Fe-doped cryptomelane has never been reported previously. The effects of different Fe^{2+} dopant concentrations are also evaluated for degradation of MB and indicated that the different Fe concentrations in the cryptomelane have an enhanced degradation of MB. The increase in the degradation of MB upon Fe doping is correlated with K^+ content, Fe/Mn ratio, crystal size, AOS of Mn and explained by the presence of more Mn^{3+} content or oxygen vacancy defects in the lattice of cryptomelane.

2 Experimental

2.1 Synthesis of the Fe-doped manganese oxide catalysts

The synthesis of the pure cryptomelane and Fe-doped cryptomelane manganese oxide materials was conducted by sol-gel method. The pure cryptomelane was prepared by a similar method reported by Ching et al. [4]. The detailed synthesis for the Fe-doped

cryptomelane-type manganese oxides is as follows: 0.033-mole citric acid was added dropwise into a purple solution of 0.1 M $KMnO_4$ under moderate stirring. The mixtures were allowed to react for 3 minutes before the addition of the different mole ratio of Fe^{2+} ($FeNO_3.9H_2O$). The sol product was immediately generated and evolved into a brown-black flocculant gel after 10 minutes of reaction time. The gel was allowed to develop in room temperature for 60 minutes, and the resultant rigid gel is filtered with 250 mL water four times and heated at 105°C for 12 hours. The solid black product is then calcined at 700°C for 5 hours, and the product was washed with HCl and DDW. The samples were dried at 110°C for overnight to generate brown gel (xerogel) and then followed by calcination at 450°C in 2 hours. The product was reduced to fine particles and washed three times with HCl 0.1 M and distilled water. The final powder product was dried at 110°C and then collected for characterization. In the synthesis process, the Fe^{2+} was added with the molar ratios of 0%, 1%, 5%, and 10% to $KMnO_4$. (The molar ratio of Fe/Mn is 0, 0.01, 0.05, or 0.10). Based on the initial molar ratio of Fe/Mn, the products were denoted as Cryptomelane, Cry (Fe 1%), Cry (Fe 5%), and Cry (Fe 10%), respectively.

2.2 Characterization methods

The various characterization techniques have been applied for the characterization of the pure and Fe-doped cryptomelane manganese oxides such as X-ray diffraction (XRD), scanning electron microscopy (SEM), atomic absorption spectroscopy (AAS). The average oxidation state (AOS) of Mn in the manganese oxide samples was determined using traditional potentiometric titration method. The X-ray patterns of all manganese oxide samples were recorded using Shimadzu XRD 7000 maxima using Cu Kα radiation (λ = 1.5406 Å) as the X-ray source. The surface morphologies of the samples were characterized using SEM JEOL JSM-6330F with acceleration potential was 15-20 kV. Samples were deposited on thin amorphous carbon films supported by copper grids from ultra-sonicated ethanol on the product. The proportion of potassium (K) and manganese (Mn) of the doped and un-doped cryptomelane was determined by atomic absorption spectroscopy (Shimadzu AA 7000). 10 mg manganese oxide catalyst was transferred into a glass beaker and added with ten mL of H_2SO_4 and diluted with DDW up to 100 mL. The mixture was then analyzed using an Atomic Absorption Spectrophotometer (SSA) to determine potassium (K) and Manganese (Mn) content.

The crystallite size of as-synthesized Fe-doped cryptomelane catalysts was estimated using Scherrer's equation:

$$D = (0.941\ \lambda) / (\beta \cos \theta) \quad (1)$$

where D was the average grain size, λ was the X-ray wavelength (0.15406), θ and β were the diffraction angles and Full-Width at Half-Maximum (FWHM, in radian) of an observed peak, respectively.

2.2 Catalytic performances of undoped and Fe-doped cryptomelane manganese oxide

The catalytic degradation reaction of MB over the manganese oxide materials was carried out in a beaker glass, which contained 25 mL of 1.6 M methylene blue, 60 mL DDW, and 1250 mg catalyst. The slurry was stirred using a magnetic stirrer at 350 rpm for 30 minutes and added 15 mL hydrogen peroxide 30%. The optical absorbance measurements were taken by pipetting eight mL aliquots of the reaction mixture at various time intervals during the reaction. The solution was immediately centrifuged for 15 min at 3000 rpm to remove

any solid particulates. Optima SP-300 Spectrophotometer was used to investigate the absorbance of the solution at a wavelength of 660 nm. The results were determined as:

$$\% \text{ decrease of MB} = \{(Co\text{-}Ct)/Co\} \times 100\ \% \quad (2)$$

2 Results and discussion

3.1 Synthesis of pure and Fe-doped cryptomelane

The XRD patterns of un-doped and Fe-doped manganese oxides are shown in Fig. 1. The oxides are typical cryptomelane-type manganese oxide with 2θ values of 12.73º, 18.09º, 23.2º, 28.69º, 32.96º, 37.5º, 41.86º, 49.85º, 55.21º, 59.92º, and 69.67º corresponding to the reflection planes of (110), (200), (220), (310), (101), (211), (301), (411), (600), (521), and (541), respectively (International centre for diffraction data no. 29-1020). No additional peaks are detected upon the incorporation of Fe^{2+} ions into pure cryptomelane, suggesting that the Fe^{2+} ions are well-incorporated into the framework of cryptomelane. Similar results are reported by Ma et al. [3] on the addition of a wide range of transition metals (Co, Fe, Ce) into the cryptomelane, where no additional peaks are observed upon dopant insertion. Gao et al. [5] reported the doping of transition metals (Cu, Ni, Co, Fe) in the cryptomelane and no new peaks are identified upon dopant addition, but the intensity of reflection peak (211) enhanced as the dopant was inserted into the cryptomelane. Shen et al. [6] reported the decrease in the intensity for (211) plane relative to (310) upon the Fe addition into cryptomelane using three different X-ray energy and explained the replacement of Mn ions in the (211) plane by Fe ions.

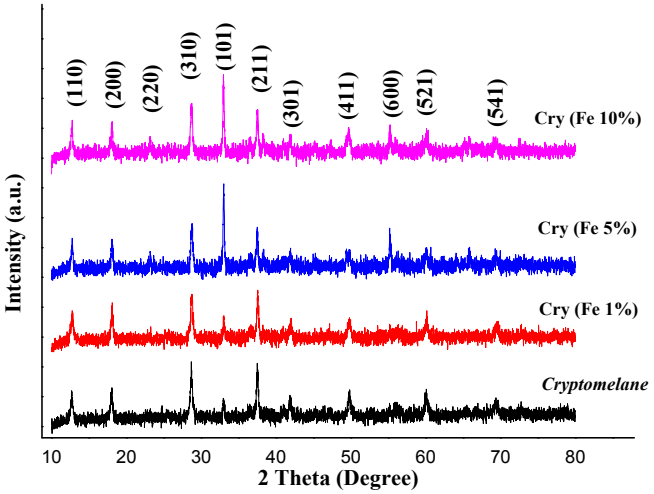

Fig. 1. The XRD patterns of pure and Fe-doped Cyptomelane-type manganese oxides.

As the Fig. 1 displayed, the intensity of (101) reflection plane increases as the Fe dopant concentration increases with the highest increase in the intensity occurred for (101) plane (the addition of 10% Fe^{2+}). These results are probably due to the rise in the distortions in the crystal lattice of cryptomelane upon increasing dopant concentration. The similar

increase in intensity for (211) reflection plane instead of the plane (101) for the doped manganese oxides was also reported by the previous study [5].

The SEM images of doped and un-doped cryptomelane are displayed in Fig. 2 which indicate that the materials show the aggregations of a particle with an irregular shape. There are no apparent differences in the morphology of the samples upon dopant insertion. This results confirmed that the distortion in the crystal structure is probably the main reason for an increase in the intensity for the plane (101). Gao et al. [5] also reported no distinct difference in the SEM images upon dopant incorporation. The results are contradicted with other studies published by Ma et al. [3] that the dopant incorporation has a significant impact on the morphology of the as-prepared doped cryptomelane. Upon Fe addition, the morphology changed from fibrous (pure cryptomelane) to chunky structure. However, when Ce is inserted into the cryptomelane, the fibrous morphology of pure cryptomelane altered to the honeycomb structure.

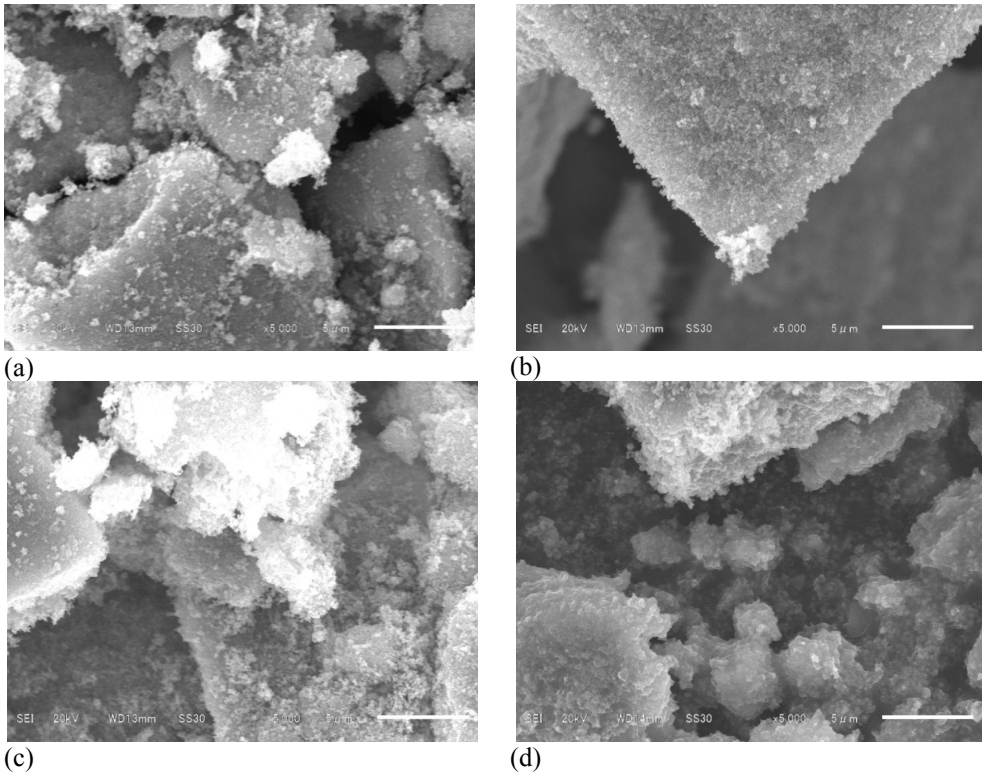

Fig. 2. The SEM images for pure cryptomelane (a), 1% Fe-doped (b), 5% Fe-doped (c), and (d) 10% Fe-doped cryptomelane.

Table 1 displayed the ratios of K/Mn and Fe/Mn, the average oxidation state of Mn, crystal size and percentage of MB degradation. The K^+ content in the tunnel of cryptomelane, in general, reduces upon Fe^{2+} ion addition, suggesting that Fe^{2+} ion replace the K^+ in the tunnel. This is confirmed by the relative constancy of the average oxidation state of Mn as the concentration of Fe^{2+} increases. The similar reduction of K^+ content and the relatively constant values of AOS of Mn in the birnessite-type manganese oxide was also observed by Qin et al. [7] upon the doping of Cu^{2+} ion.

Table 1. Elemental analysis, AOS, crystal size and % MB degradation.

Catalyst	K/Mn	Fe/Mn	AOS before Deg.	Crystal size (nm)	MB degradation (%)
Fe 0%	0.67	0.00	3.75	9.601	54.820
Fe 1%	0.80	0.02	3.80	16.666	60.861
Fe 5%	0.46	0.21	3.87	24.848	77.828
Fe 10%	0.55	0.09	3.90	33.040	59.056

3.2. The catalytic activities of Pure and Fe-doped cryptomelane

The catalytic performance of the pure cryptomelane and Fe-doped cryptomelane on the degradation of MB dye has been studied in the presence of hydrogen peroxide. It can be seen from Fig. 3 that with the addition of pure cryptomelane, only 30% MB degradation occurred at 10 minutes of reaction times. The addition of 1% Fe into pure cryptomelane leads to 40% MB degradation with the similar reaction time. Further increase in Fe doping (5% Fe) results in the significant improvement in the MB degradation with 58% of MB degradation being achieved with 10 minutes of reaction time. For 10% Fe, however, the MB degradation is reduced to 40% with 10 minutes of reaction time, which is similar to the MB degradation for 1% Fe. Thus, there is a certain limit for Fe content in the Fe-doped cryptomelane for the improvement of MB degradation. The saturated degree of MB degradation for 5% Fe was achieved as high as 77.8% for 120 minutes of reaction time. The K^+ content has been reported to play a significant role in the catalytic activity of cryptomelane. The K^+ ions intercalated into an interlayer of a birnessite or in tunnel cryptomelane are correlated with the concentration of oxygen vacancy defect or Mn^{3+} content in a cryptomelane or birnessite (octahedral layered manganese oxide) according to the reaction [8]:

$$Mn^{4+}O^{2-}{}_2 + xK^+ \rightarrow K^+{}_xMn^{4+}{}_{1-x}\,Mn^{3+}{}_xO^{2-}{}_2 \quad (3)$$

$$-\,Mn^{4+}\text{–}O^{2-}\text{–}Mn^{4+}\text{–} \;\rightarrow\; -\,Mn^{3+}\text{–}\square\text{–}Mn^{3+}\text{–} + \tfrac{1}{2}\,O_2 \quad (4)$$

The overall reaction can be written as follows:

$$Mn^{4+}O^{2-}{}_2 + xK^+ \rightarrow K^+{}_xMn^{4+}{}_yMn^{3+}{}_{1-y}O^{2-}{}_{2-z} + {}^z/_2\,O_2 \quad (5)$$

where $y = 1 - x - 2z$, and $\square$ is the oxygen vacancy created due to the presence of Mn^{3+}.

In this work, the K^+ content reduced into the lowest point for 5% Fe, indicating the presence of more oxygen defect in Fe-doped cryptomelane, which in turn enhanced the catalytic activity of Fe-doped cryptomelane. The crystal size of Fe-doped cryptomelane samples increases as the dopant concentration increases, with the highest increase obtained for the Fe 10%, which is 33.040 nm. Usually, the smaller crystal size means that higher surface area of a material with the same weight, which leads to the more adsorption and reaction to occur on the surface of the material. In this case, the size of the crystal is not the dominant factor for the degradation of MB over the Fe-doped cryptomelane catalysts.

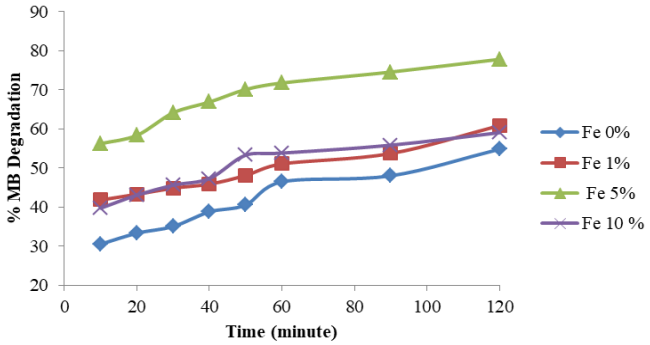

Fig. 3. Percentage of MB degradation over pure and Fe-doped cryptomelane with condition of reaction: initial concentration of [MB] = 4.8 mol/L, volume of [H_2O_2] = 15 mL, amount of cryptomelane catalysts = 0.05 g/L.

4 Conclusions

The as-synthesized Fe-doped cryptomelane-type octahedral molecular sieve manganese oxides have been successfully synthesized by a facile redox reaction by reacting the whole reactants in one vessel using a sol-gel method. The as-prepared doped materials show the aggregation of particles with irregular shapes as shown by SEM images, which are similar to the pure cryptomelane. The XRD patterns of Fe-doped cryptomelane display the same reflection planes as the pure cryptomelane, except the more intense peak for (101) reflection plane, indicating the distortion of crystalline nature upon dopant addition. The as-synthesized Fe-doped cryptomelane-type octahedral molecular sieve manganese oxides show higher catalytic activities for MB degradation compared to the pure cryptomelane, which is probably due to the higher oxygen vacancy defect.

This work was supported by the Ministry of Research-Technology and Higher Education, the Republic of Indonesia under the scheme of Advanced Material Research with the contract no. 358/UN.19.5.1.3/PP/2018. The author also thanks the Department of Chemistry, Universitas Riau for providing the facilities for conducting this research.

References

1. P.V. Nidheesh, R. Gandhimathi, S.T. Rames, Env. Sci. Pollut. Res. **20** (2013)
2. A. Awaluddin, M. Agustina, R.R. Aulia, Muhdarina. *Proc. of International Conference on Chemistry, Chemical Process and Engineering (IC3PE)* **020108** (2017)
3. J. Ma, C. Wang, H. He, Appl. Catal. B, Env. **201** (2017)
4. S. Ching, J.L. Roark, N. Duan, S.L. Suib, Chem. Mat. **4756** (1997)
5. J. Gao, C. Jia, L. Zhang, H. Wang, Y. Yang, S.F. Huang, Y.Y. Hsu, B. Liu, J. Catal. **341** (2016)
6. X. Shen, A.M. Morey, J. Liu, Y. Ding, J. Cai, J. Durand. Q. Wang, W. Wen, W. A. Hines, J. C. Hanson, J. Bai, A. I. Frenkel, W. Reiff, M. Aindow, S. L. Suib, J. Phys. Chem. C **115,** 21610–21619 (2011)
7. Z. Qin, Q. Xiang, F. Liu, J. Xiong, L.K. Koopal, L. Zheng, M.G. Vogel, M. Wang, X. Feng, W. Tan, H. Yin, Chem. Geol. **466** (2017)
8. J. Hou, Y. Li, M. Mao, L. Ren, X. Zhao, ACS Appl. Mat. Interfaces **6** (2014)